Electronic Supporting Information

Conductive Zn(II)-metallohydrogels: Role of alkali metal cations size over gelation, rheology and conductance

Chinthakuntla Mahendar,[a] Yeeshu Kumar,[a] Manish Kumar Dixit,[a] Moupia Mukherjee,[a] Abul Kalam[b] and Mrigendra Dubey*[a]

[a]Soft Materials Research Laboratory, Department of Metallurgy Engineering and Materials Science, Indian Institute of Technology Indore, Indore-453552, India

[b]Department of Chemistry, College of Science, King Khalid University, Abha 61413, Saudi Arabia

***Email:** mdubey@iiti.ac.in, mrigendradubey@gmail.com*

Table of Contents: **Pages**

EXPERIMENTAL SECTION

Synthesis and characterization:

(10E, 15E)-N$^{1'}$,N$^{4'}$-bis(2-hydroxybenzylidene)trephthalohydrazide (*o*-H$_4$TEP)

Terephthalohydrazide was synthesized from dimethyl terephthalte and hyrazine hydrate by following litrature.[1] Methanolic solution of 2-Hydroxybenzaldehyde (0.628 g, 5.15 mmol) was added dropwise to suspension of terephthalohydrazide (0.500 g, 2.577 mmol) in methanol. Further, the resulting suspension was refluxed for 5-6 hours at 60^{o}C to complete the reaction. It afforded white coloured soild compound which was washed with methanol, water and Diethyl Ether and dried in vacuum. Yield 1.0 g (88%). ^{1}H NMR (DMSO-d_6, 400 MHz, ppm) δ_H 7.14 (d, 4H, Ar), 7.51 (t, 2H, Ar), 7.77 (d, 2H, Ar), 8.28 (s, 4H, Ar), 8.87 (s, 2H, =CH), 11.40 (s, 2H, OH) and 12.42 (s, 2H,-NH).

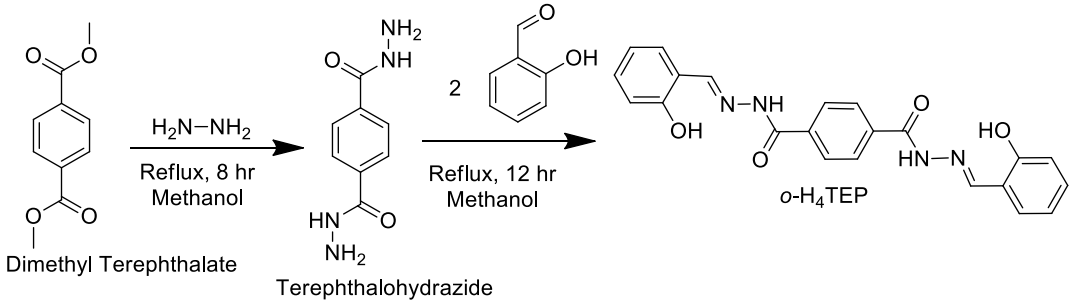

Scheme S1: Synthetic route addopted for the synthesis of ***o*-H$_4$TEP**.

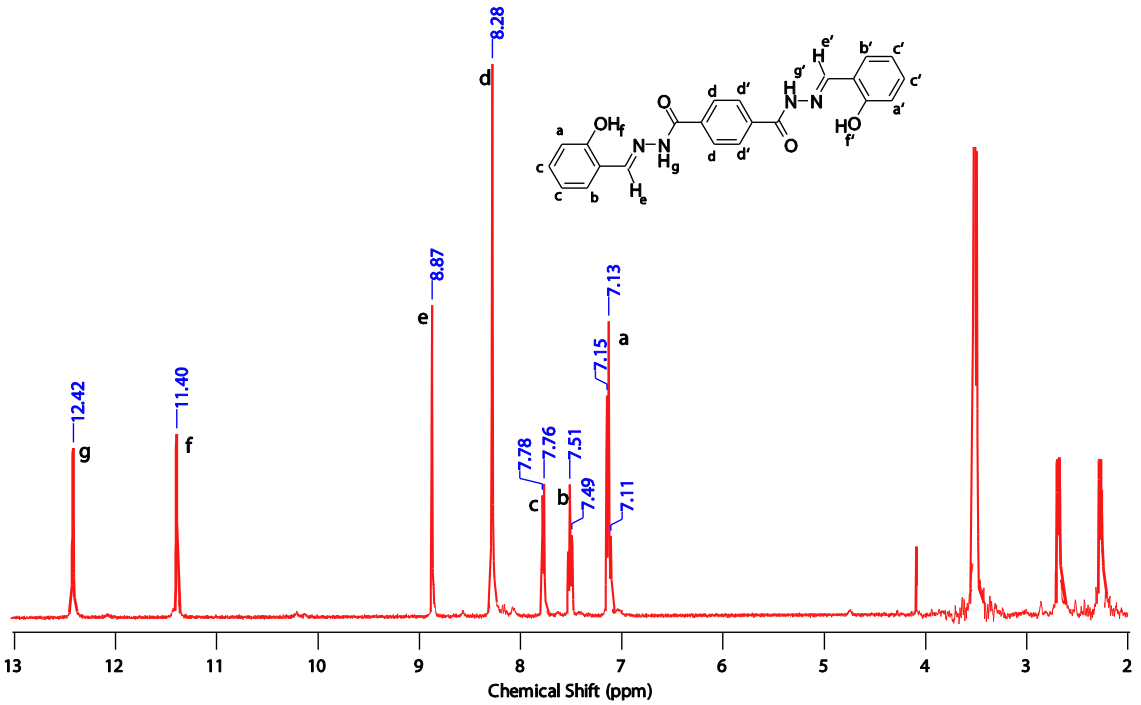

Figure S1. ^{1}H NMR Spectra of ***o*-H$_4$TEP** in DMSO-d_6, 400 MHz, ppm.

Table S1: Gelation tests in various common laboratory solvents*

S. N.	Solvent	*o*-H_4TEP/ LiOH/ $Zn(NO_3)_2$
1.	Water	**G**
2.	Acetonitrile	S
3.	Methanol	p
4.	Ethanol	p
5.	DMF	S
6.	DMSO	S
7.	Acetone	S
8.	Chloroform	S
9.	DCM	S
10.	THF	S

*Where, S= solution, G= gel, P= precipitate.

Table S2: Gel or sol formation of ***o*-H_4TEP** in presence of $Zn(NO_3)_2$ with different alkali bases*

Solvent	1+LiOH	1+NaOH	1+KOH	1+CsOH
H_2O	**G**	G	G	G

*Where, G= gel.

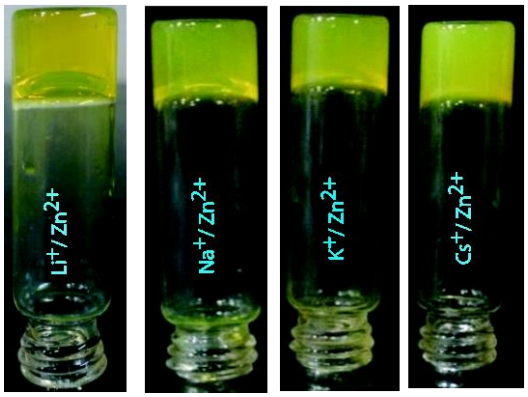

Figure S2. Picture represents the gelation ability of ***o*-H_4TEP** with (A) Li^+, (B) Na^+, (C) K^+ and (D) Cs^+.

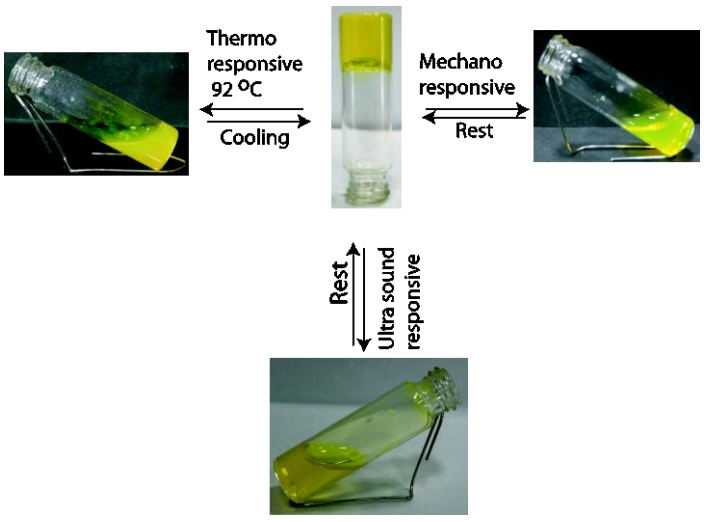

Figure S3: Stimuli responsive properties of **MH-Li** metallogel.

Table S3: Screening of gelation behaviour of ***o*-H_4TEP** +LiOH in presence of different transition metal nitrates

Solvent	$Co(NO_3)_2$	$Cu(NO_3)_2$	$Fe(NO_3)_2$	$Cd(NO_3)_2$	$Zn(NO_3)_2$
H_2O	P	P	P	P	G

*Where, G= gel and P= precipitate.

Table S4: Effect of Counter anions on gel formation in presence of ***o*-H_4TEP/LiOH**

Solvent	$Zn(OAc)_2$	$ZnCl_2$	$Zn(ClO_4)_2$	$ZnSO_4$	$Zn(NO_3)_2$
H_2O	P	P	P	P	G

*Where, G= gel and P= precipitate.

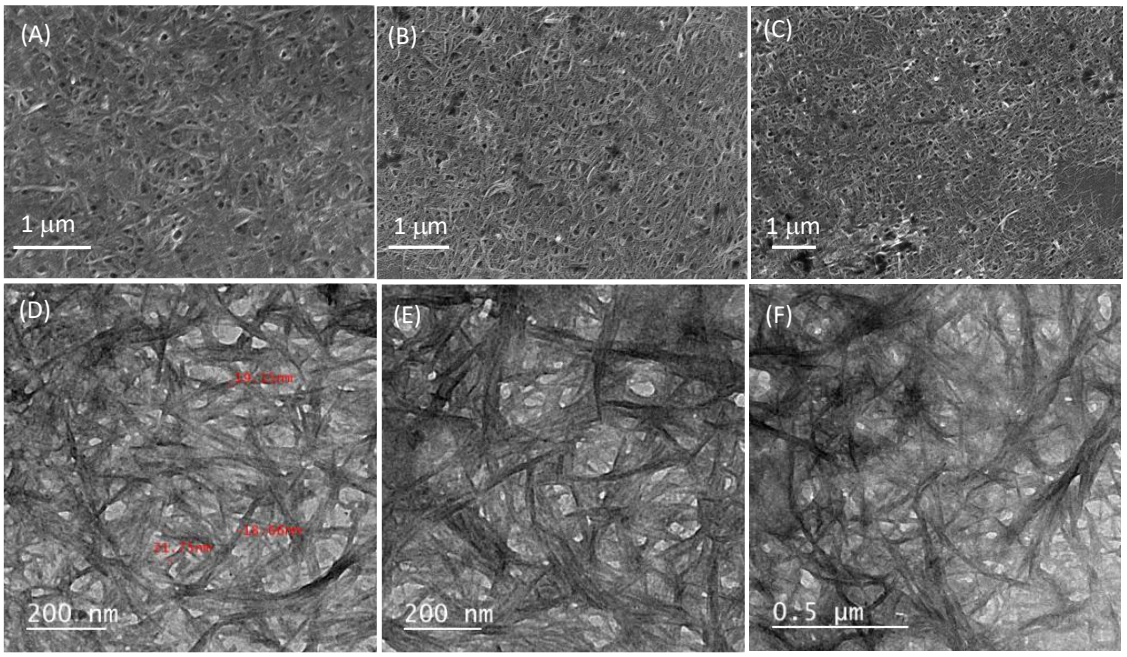

Figure S4. MH-Li : (A-C) FE-SEM and (D-F) TEM at different maginifications.

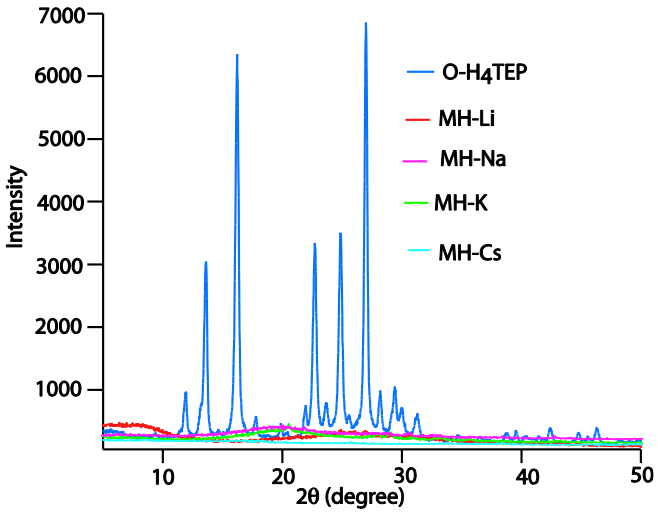

Figure S5. PXRD pattern of ***o*-H_4TEP** (Blue line), **MH-Li** (Red line)**, MH-Na** (Pink line)**, MH-K** (Green line) **and MH-Cs** (Sky Blue line) xerogels.

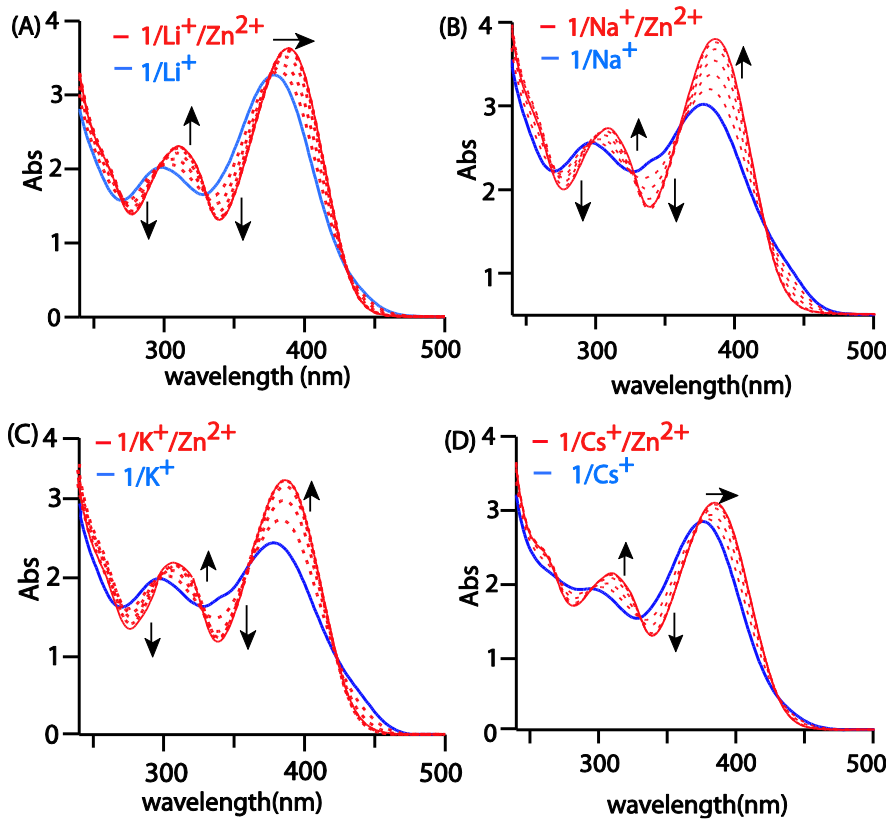

Figure S6. UV-vis titration experiments of (A) LiOH, (B) NaOH, (C) KOH and (D) CsOH deprotonated ***o*-H_4TEP** (1) ($1X10^{-4}$M, H_2O) with 2 equivalents of $Zn(NO_3)_2$ ($1X10^{-2}$M, H_2O).

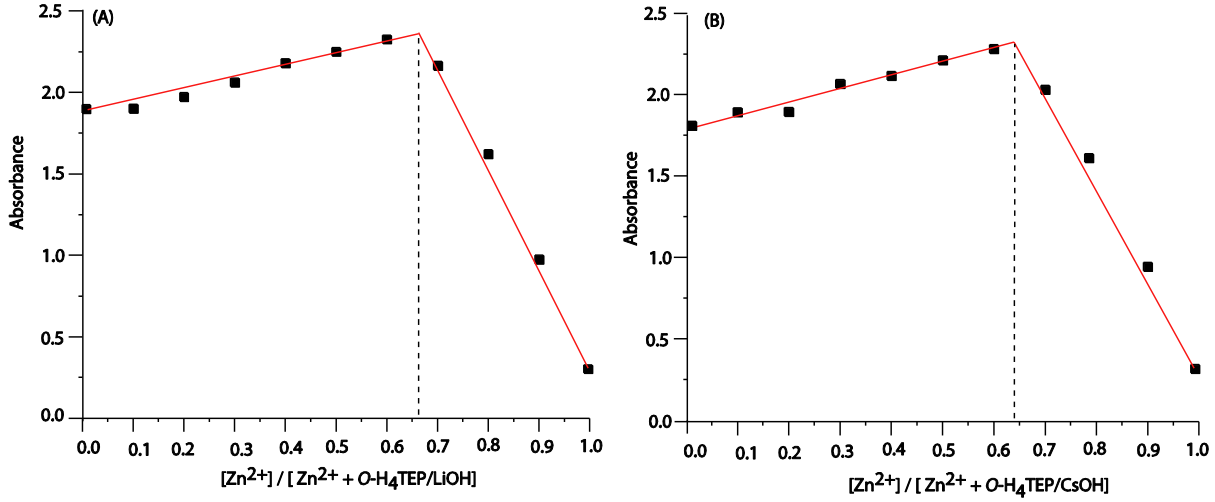

Figure S7. Job's plot for **(A)** LiOH deprotonated ***o*-H_4TEP** *vs* $Zn(NO_3)_2$ **(B)** CsOH deprotonated ***o*-H_4TEP** vs $Zn(NO_3)_2$.

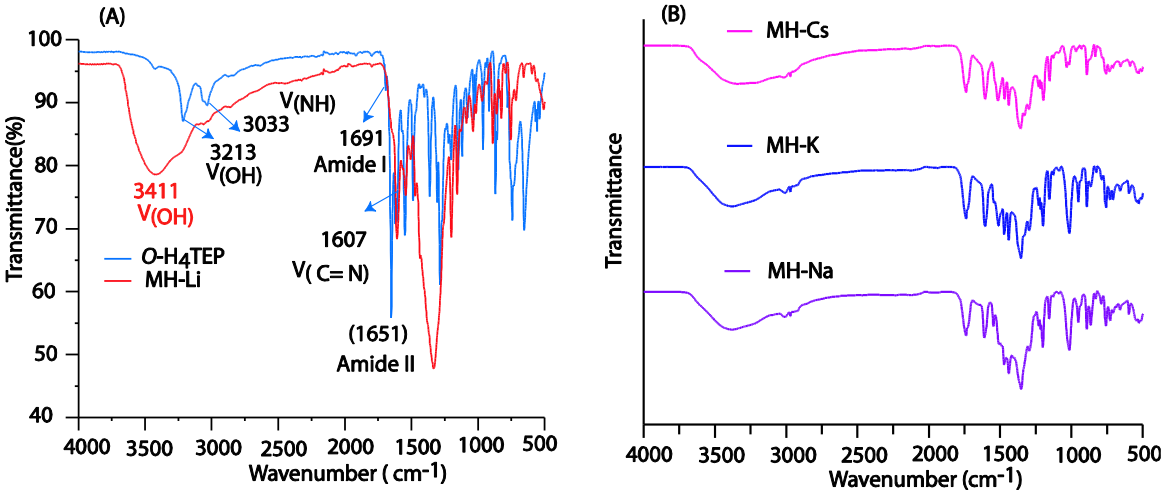

Figure S8. FT-IR spectra of (A) ***o*-H$_4$TEP** and **MH-Li** xerogel (B) **MH-Na**, **MH-K**, **MH-Cs** xerogels.

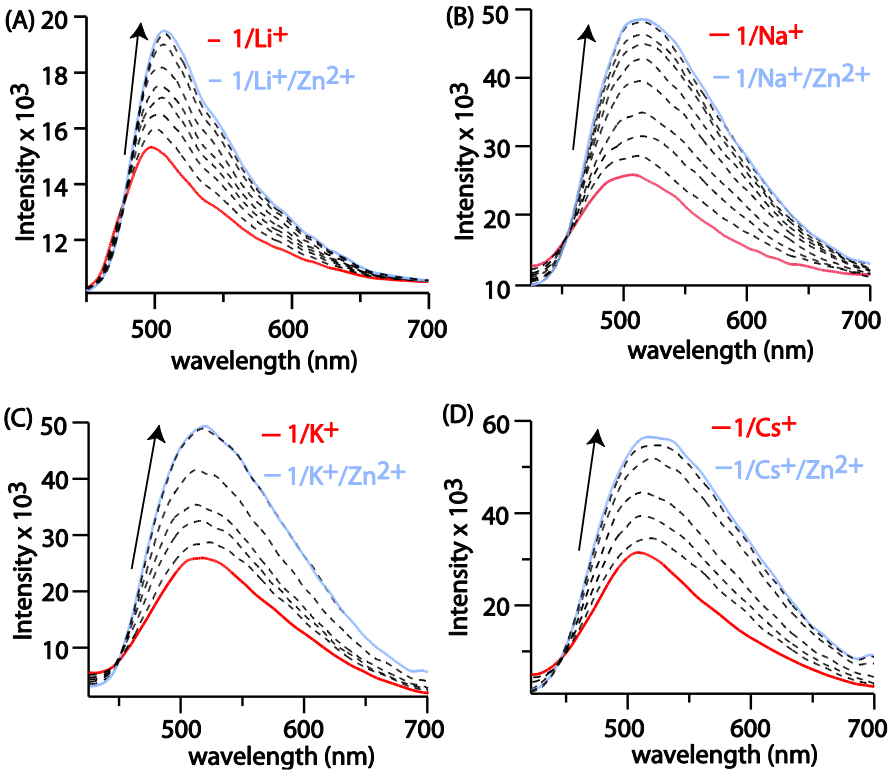

Figure S9: Fluorescence titration of alkali base (A). Li^+, (B). Na^+, (C). K^+, (D). Cs^+ deprotonated ***o*-H$_4$TEP** (10^{-4} M) with $Zn(NO_3)_2$ (10^{-2}M).

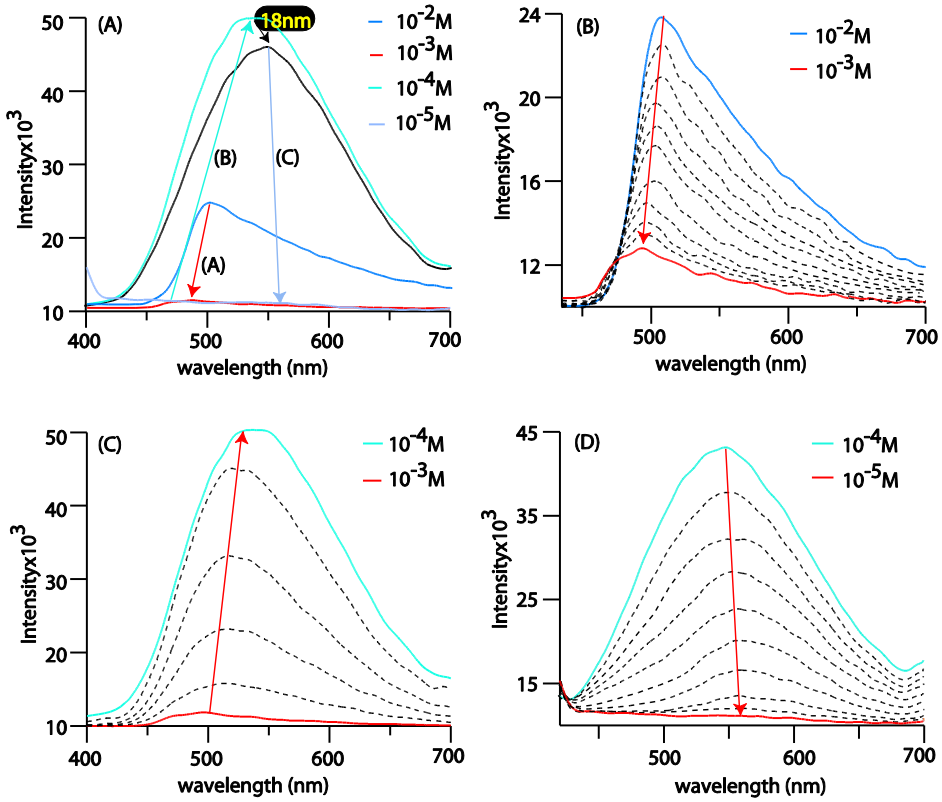

Figure S10: Fluorescence dilution experiment of MH-Li Gel: (A) complete comparative dilution analysis, 18 nm red shift was observed upon dilution from 1x 10^{-4} M to 0.85X10-4 M, represented in black line (B) Dilution from 10^{-2}M to 10^{-3}M shows presence of CHEFF phenomenon, (C) Dilution from 10^{-3}M to 10^{-4}M shows presence of ACQ phenomenon and (D) Dilution from 10^{-4}M to 10^{-5}M shows dilution effect.

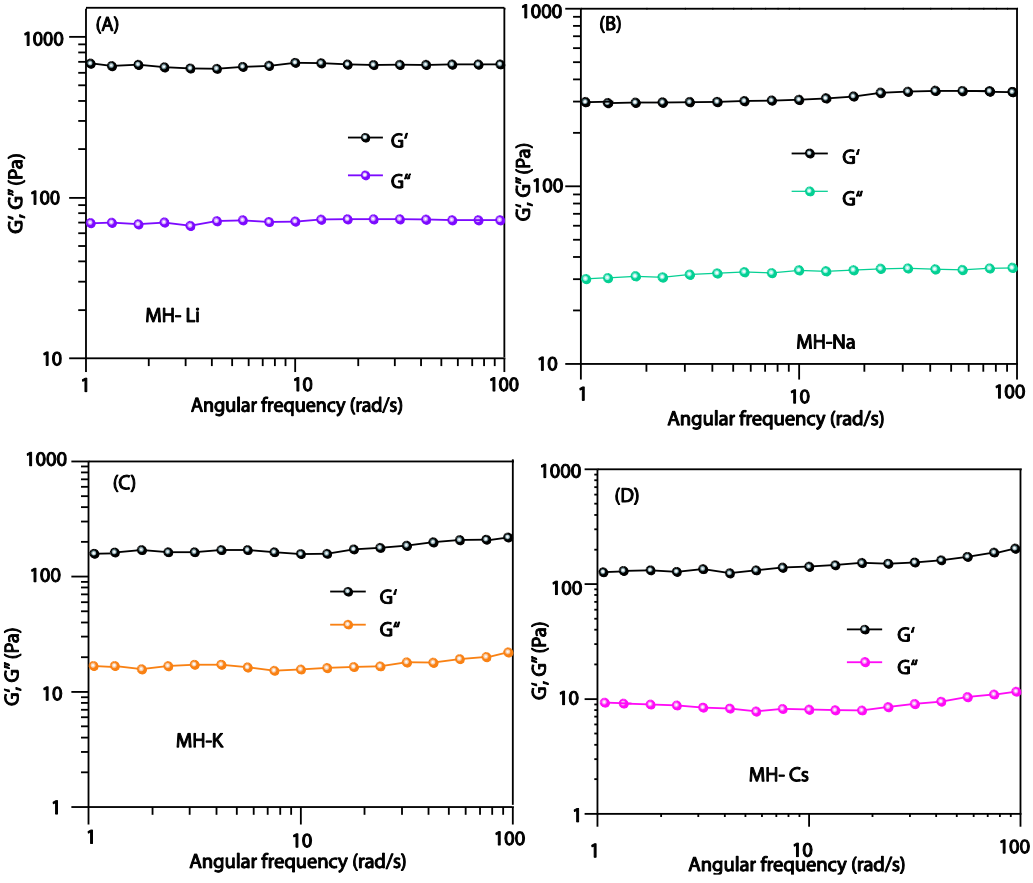

Figure S11. Dynamic Frequency Sweep: (A) MH-Li (B) MH-Na (C) MH-K and (D) MH-Cs.

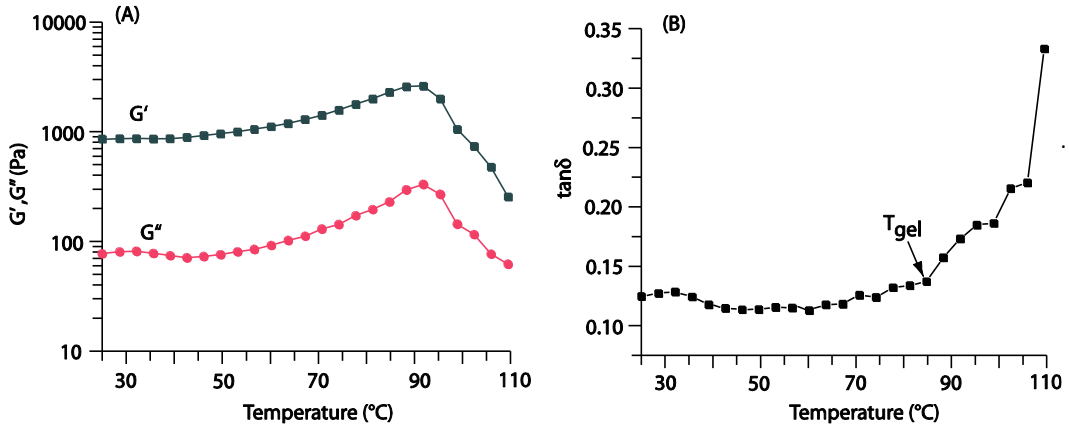

Figure S12. (A) Dynamic temperature ramp over the loss modulus (G″) and storage modulus (G′) for **MH-Li**, **(B)** Plot of tan δ vs. temperature and T_{gel} = 85 °C.

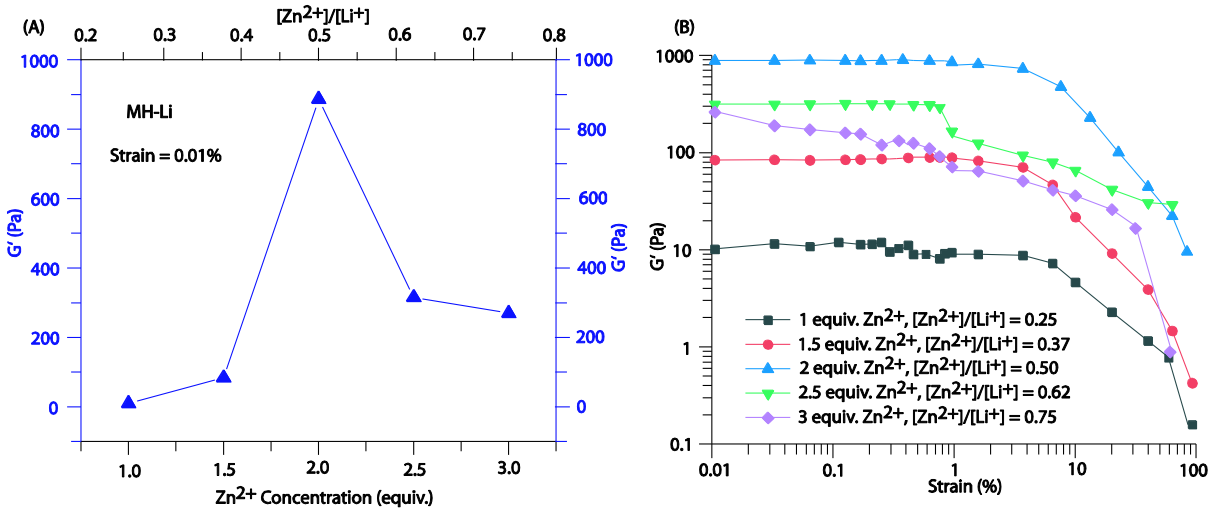

Figure S13. Effect of [Zn^{2+}] concentration on the rheological properties of MH-Li; (A) plot the G′ values against the concentration of Zn^{2+} along with the ratio of [Zn^{2+}]/[Li^{+}] at 0.01 % strain and (B) Plot of G′ vs strain at various Zn^{2+} concentrations.

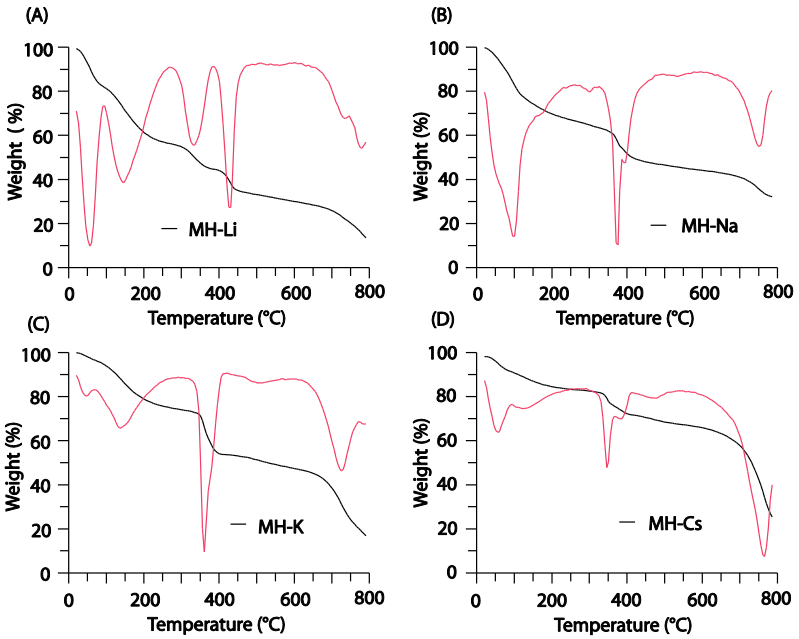

Figure S14. The Thermo Gravimetric Analysis (TGA) along with derivative plot for (A) **MH-Li** (B) **MH-Na** (C) **MH-K** and (D) **MH-Cs** xerogels.

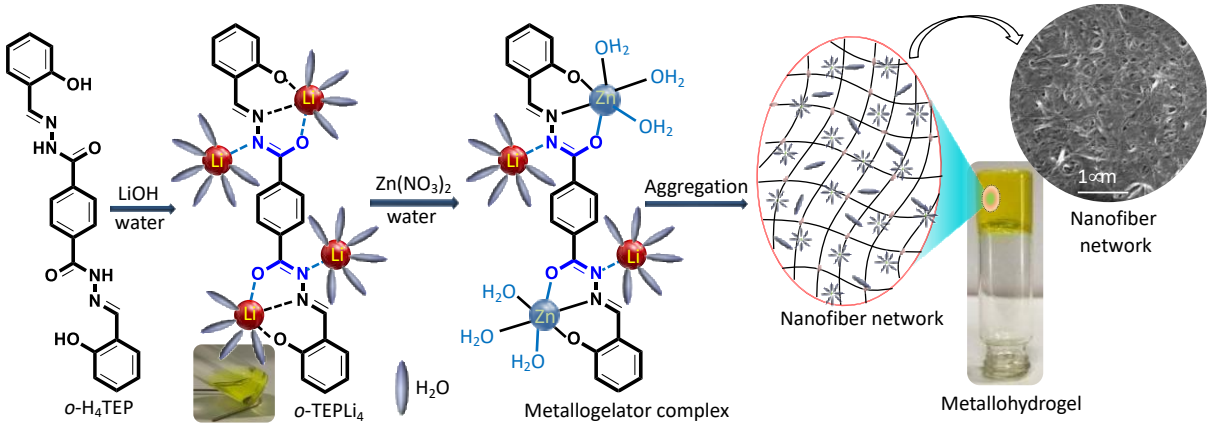

Figure S15. Pictorial representation of steps involved in gelation process.

References:

1. M. Dubey, A. Kumar, R. K. Gupta and D. S. Pandey, *Chem. Commun.,* 2014, **50**, 8144.